



# Reflectances of SPOT multispectral images associated with the turbidity of the Upper Gulf of California

Aguilar-Maldonado, J. A.\*<sup>1</sup>, Santamaría-del-Ángel, E.\*<sup>1</sup>, Sebastián-Frasquet, M. T.<sup>2</sup>

<sup>1</sup> *Facultad de Ciencias Marinas. Universidad Autónoma de Baja California, Mexico.*

<sup>2</sup> *Instituto de Investigación para la Gestión Integrada de Zonas Costeras. Universitat Politècnica de València, España.*

**Abstract:** The use of satellite images for the observation and measurement of marine turbidity has been developed mainly with ocean colour sensors, such as MODIS. These images have a maximum spatial resolution of 250 m in their visible and infrared bands. In this research, images of the SPOT sensors were chosen as an alternative to overcome this limited spatial resolution. The objective was to prove the suitability of SPOT to measure turbidity in areas with great spatial variability. As a first step, all the images were standardized and the SPOT wavelength that had the largest association in the Principal Component Analysis was chosen (PCA). The results show that the bands of a SPOT multispectral image are highly redundant. The wavelength of the 610-680 nm ( $S2_{610-680}$ ) obtained the best association in 89% of the 73 images analysed. The SPOT reflectance ( $R_{rs}$ ) ( $S2_{610-680}$ ) was compared with MODIS 620-670 nm ( $M1_{620-670}$ ), which has already been tested in other research and has proved to be adequate for measuring turbidity. Both sensors performance was similar for low and moderate reflectance but for high reflectance, SPOT ( $S2_{610-680}$ ) had a better performance than MODIS ( $M1_{620-670}$ ). Additionally, the SPOT  $R_{rs}$  ( $S2_{610-680}$ ) was associated with standardized Secchi disk depth data, which were measured *in situ*, to check SPOT suitability. SPOT  $R_{rs}$  ( $S2_{610-680}$ ) images were classified into: 1) cold or warm season, 2) spring tide or neap tide and 3) water flux or reflux. These constructed scenarios allowed to see the result of the Standardized Space Anomalies, which showed the continuous presence of low and medium values in the most oceanic region of the Upper Gulf of California (UGC) and very high values in all the scenarios in the intertidal zone. This research has shown that SPOT  $R_{rs}$  ( $S2_{610-680}$ ) is useful for observing, differentiating and measuring turbidity patterns in areas with very high spatial variability.

**Key words:** Upper Gulf of California, Colorado River Delta, Turbidity, Multispectral images, SPOT, MODIS, Secchi Disk.

## Reflectancias de imágenes multiespectrales de SPOT asociadas a la turbidez en el Alto Golfo de California

**Resumen:** El uso de imágenes de satélite para la observación y medida de la turbidez marina se ha desarrollado principalmente con sensores de color del océano como MODIS. Estas imágenes tienen una resolución espacial máxima de 250 m en las bandas visible e infrarroja. En esta investigación, se eligieron imágenes del sensor SPOT como alternativa para superar esta limitada resolución espacial. El objetivo es probar la validez de SPOT para medir turbidez en áreas con gran variabilidad espacial. Como primer paso se normalizaron todas las imágenes y se eligió la longitud de onda de SPOT que mejor ajuste obtuvo a partir del Análisis de Componentes Principales (ACP). Los resultados mostraron que las bandas de una imagen multiespectral SPOT tienen una alta redundancia (buena correlación) entre sí. La longitud de onda de los 610-680 nm ( $S2_{610-680}$ ) fue la que obtuvo el mejor ajuste en 89% de las 73 imágenes

**To cite this article:** Aguilar-Maldonado, J. A., Santamaría-del-Ángel, E., Sebastián-Frasquet, M. T. 2017. Reflectances of SPOT multispectral images associated with the turbidity of the Upper Gulf of California. *Revista de Teledetección*, 50, 1-16. <https://doi.org/10.4995/raet.2017.7795>

\* *Corresponding author: [jesusaguilarmaldonado@gmail.com](mailto:jesusaguilarmaldonado@gmail.com), [santamaria@uabc.edu.mx](mailto:santamaria@uabc.edu.mx)*

analizadas. Esta reflectancia ( $R_{rs}$ ) ( $S2_{610-680}$ ) de SPOT fue comparada con MODIS ( $M1_{620-670}$ ). El comportamiento de ambos sensores fue similar para reflectancias bajas y medias, pero para altas reflectancias SPOT  $R_{rs}$  ( $S2_{610-680}$ ) tuvo un mejor rendimiento que MODIS. Además, la  $R_{rs}$  ( $S2_{610-680}$ ) de SPOT fue asociada con datos *in situ* normalizados de profundidad del disco de Secchi para comprobar la idoneidad del sensor SPOT. Las imágenes  $R_{rs}$  ( $S2_{610-680}$ ) de SPOT fueron clasificadas en: 1) época fría o cálida, 2) marea viva o muerta, y 3) flujo o refluo de las aguas. Estos escenarios seleccionados permitieron ver el resultado de las Anomalías Espaciales Normalizadas, que dejaron ver la continua presencia de valores bajos y medios en la región más oceánica del Alto Golfo de California (AGC) y valores muy altos en todos los escenarios en la zona intermareal del AGC. El trabajo realizado permite concluir que la reflectancia  $R_{rs}$  ( $S2_{610-680}$ ) de SPOT es válida para observar, diferenciar y medir patrones de turbidez en áreas con una elevada variabilidad espacial.

**Palabras clave:** Alto Golfo de California, Delta del Río Colorado, Turbidez, Imágenes multiespectrales, SPOT, MODIS, Disco de Secchi.

## 1. Introduction

In ocean remote sensing monitoring, optically complex waters are defined as those that have an important influence not only of phytoplankton and related elements, but also of other substances, such as inorganic particles in suspension and dissolved organic matter (IOCCG, 2000). In very turbid water, dispersion of the incident light by the Suspended Particulate Matter (SPM) may have an inhibitory effect on primary production (Gordon and McCluney, 1975). Thus, the knowledge of distribution and variability of turbidity in coastal waters is important for understanding some biological processes (Doxaran *et al.*, 2002).

Likewise, turbidity estimation is important to quantify the rivers contribution of sediments to the ocean (Froidefond *et al.*, 1991; Anji Reddy, 1993; Forget *et al.*, 1999; Moore *et al.*, 1999; Doxaran *et al.*, 2002). The role that these contributions play in the marine ecosystem is fundamental both for the maintenance of productivity and for the survival of delicately balanced ecosystems such as the deltas. In addition, the quantification of turbidity can also provide very useful information for the management and planning of dredging in ports, canals and navigable estuaries (Gippel, 1995; Doxaran *et al.*, 2006).

The cost of *in situ* marine monitoring programs, developed to identify the natural variability in water quality parameters (such as turbidity), is very high. There are very few places that have monitoring programs with continuity, at best with monthly or bi-monthly frequency (for example the marine monitoring network for Latin America Antares

(www.antares.ws), the cooperation network for the Northeast Atlantic OSPAR (www.ospar.org), The Bermuda's Atlantic Time Series BATS (<http://bats.bios.edu/>) and Hawaii Ocean Time-series HOT (<http://hahana.soest.hawaii.edu/hot/>) or four-monthly (for example, the California Current Marine Monitoring Network CALCOFI (www.calcofi.org). In addition, *in situ* sampling generally leads to underestimation of loads and requires too high sampling frequency to characterize temporal trends (Gippel, 1995; Nechad *et al.*, 2010). Remote sensors are a valuable tool for identifying and monitoring the distribution of suspended sediments at a lower cost and more frequently, allowing to build a synoptic description of the variability of turbidity patterns (Nechad *et al.*, 2010).

In this sense, MODIS, Terra and Aqua sensors, images have been used in research to determine the spatio-temporal variability of turbidity concentrations from their reflectances ( $R_{rs}$ ) at a maximum spatial resolution of 250 m (Dogliotti *et al.*, 2011; Shi and Wang 2007; Wang and Shi, 2005). In these sensors, band has been associated with three optical properties: light transmittance in the water column, Secchi disk depth transparency and nephelometric turbidity, in the Bay of Biscay (Chust *et al.*, 2006).

Other images, such as Landsat, have been tested to improve spatial resolution. Landsat images have been associated with radiance (Doxaran *et al.*, 2006), and signal penetration at different depths (Gordon and McCluney, 1975; Anji, 1993; Baeye *et al.*, 2016; Lee *et al.*, 2016). These images have been used to detect and quantify surface turbidity

in estuaries (Ackleson *et al.*, 1985; Gernez *et al.*, 2015, Jalón-Rojas *et al.*, 2015 y Cai *et al.*, 2015). Otherwise, SPOT images have been tested in optically complex waters to locate maximum concentrations of suspended material and areas of erosion and deposition (Doxaran *et al.*, 2002, 2006). This information can be obtained because turbidity plays as a tracer of current, and allows to observe hydrodynamic characteristics. Continuous use of high-resolution images allows detailed descriptions of tidal turbidity at multi-year time scales (Jalón-Rojas *et al.*, 2016).

The objective of this work was to identify the SPOT band wavelength which reflectances may be useful to detect and quantify turbidity level in marine waters, validating the use of SPOT, comparing it with MODIS and taking Zsecchi *in situ* data. To test SPOT effectiveness in describing temporal turbidity patterns for different scenarios (season, tidal conditions, flow conditions) in coastal areas of optically complex waters.

## 2. Materials and methods

### 2.1. Study area

This research was developed in the Upper Gulf of California (UGC) and Colorado River Delta (CRD) (Baja California, Mexico) (Figure 1). This area has several protection figures; among them it was declared as Biosphere Reserve in 1993. In addition, it is the habitat of endangered species, such as totoaba (*Totoaba macdonaldi*) and vaquita (*Phocoena sinus*) (Santamaría-del-Ángel *et al.*, 1994; Santamaría-del-Ángel 2017). This region is especially important for the reproduction, breeding and development of marine species economically important, such as shrimp and yellow mouth croaker. This area is specially characterized by high concentrations of nutrients (Hernández-Ayón *et al.*, 2013) and high primary productivity, which holds a large food chain with high biomass in each of its levels, and thus, maintain high fishing activity (Santamaría-del-Ángel *et al.*, 1996; Millán-Núñez *et al.*, 1999; CONANP, 2007; Mercado-Santana *et al.*, 2017). Despite very high irradiances values in the area (Bastidas-Salamanca *et al.*, 2014), the high turbidity values limit the euphotic zone (Millán-Núñez *et al.*, 1999). It has been reported that the phytoplankton communities

presents adaptation strategies to this limited photic layer and a temporal space variability that is presumed to be linked to the turbidity patterns present in this area (Santamaría-del-Ángel *et al.*, 1996). So, understanding the turbidity patterns is key for this type of coastal ecosystems, because it regulates the base of the food chain, and therefore all the processes that derive from this (Doxaran *et al.*, 2002).

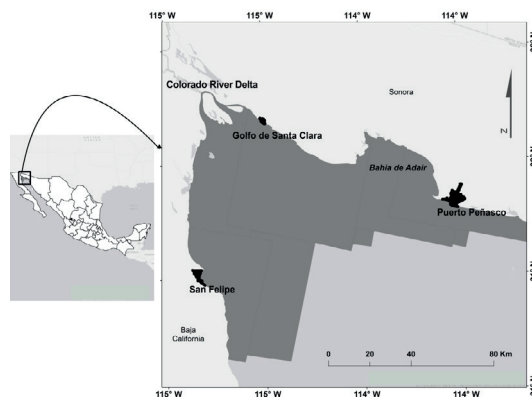


**Figure 1.** Study area location, Upper Gulf of California and Colorado River Delta (Baja California, Mexico). The dark grey area was covered with SPOT images from year 2008 to 2013. Tide stations used in this study were located in Golfo de Santa Clara, San Felipe and Puerto Peñasco coastal towns.

### 2.2. Processing of SPOT images

In this study we used 73 SPOT images of the sensors 2, 4, 5 and 6 of the period between 2008 and 2013. The following corrections were applied to images 1) radiometric correction, the images were compensated for sensor defects, variations in scanning angle and system noise at the time the image was produced, based on the number of pixels and the band number of each image (Le Gall *et al.*, 2010; Lira-Chávez, 2010); 2) atmospheric correction, the Fast Line-of-Sight Spectral Hypercubes Atmospheric Analysis (FLAASH) model was used (Griffin and Burke, 2003), and the Marine Model was used to correct the visible wavelengths with the regions of the near infrared and the regions of infrared shortwave (Kaufmann *et al.*, 1991; Abreu and Anderson, 1996; Berk *et al.*, 1999; Matthew *et al.*, 2000); and 3) geometric correction, to homogenize images parameters to an UTM projection zone 11, with Datum WGS84 (NIMA, 2000).

### 2.3. SPOT comparison with MODIS

In order to compare the images of MODIS and SPOT, SPOT multispectral images, which are at a resolution of 10 or 20 meters (Table 1), were converted to the same spatial resolution as the visible band  $M1_{620-670}$  of MODIS, which is 250 meters. In addition, they were taken to a radiometric resolution of 8 bits to be able to have an image with 256 values ( $2^8=256$ ), ranging from 0 to 255 and related to the values of the MODIS images. According to Lira-Chavez (2010), the reason for using 256 levels is that this number is stored in an 8-bit byte of a digital computer, in addition to generating a 255 for the brightest instantaneous field of view (IFOV) of the scene, and a 0 for the darkest.

The SPOT images used were from the coastal area of the UGC. In order to avoid confusion in the bands reflectance signal, the terrestrial area was masked, leaving only the sea area. This makes it possible to better distinguish the  $R_{rs}$  from the four bands of each of the SPOT images on the water body.

### 2.4. Assessment of SPOT sensors wavelengths

In order to determine which wavelength, and therefore which SPOT band, is most adequate to determine turbidity, we performed a PCA according to Santamaria-del-Ángel et al., (2011b) criteria. Table 1 shows the spectral characteristics of the SPOT sensor bands used in this work.

According to Lira-Chavez (2010), there is an association between the bands of a multispectral image, in particular when these are contiguous. For close energy intervals the corresponding information is similar. In other words, between adjacent bands there is a redundancy of information, which

means that the covariance matrix of the original image has elements other than zero outside the diagonal. As the “eigenvalues” are arranged decreasingly, the information content of the image is redistributed among the components so that more information is concentrated in the first component or bands of the output image, while the remaining one has very little information and virtually all the noise contained in the original image. From the correlation matrix is derived the numerical resolution of the PCA, the Principal Components (PC) associated with the image bands, which were calculated as Standardized Empirical Orthogonal Functions (SEOF). This transformation is unitary and is therefore considered as an overall enhancement to the image. Its advantage is that it does not require input parameters, but only uses the statistical properties of the multispectral image set. In addition, each output band can have a physical interpretation, since the associated eigenvectors and eigenvalues have it.

In order to obtain comparable data between the SPOT bands, the MODIS data and the measurements “*in situ*”, the pixel values of the SPOT bands were standardized according to Santamaria-del-Ángel et al., (2011b).

### 2.5. SPOT scenario construction (mosaics)

SPOT images were classified according to oceanic conditions at the moment of the scene (neap or spring tide, in flux or in reflux, warm or cold season), in order to be able to study the turbidity in different conditions. Testing turbidity in different conditions will allow to prove the hypothesis that at higher turbidity higher the  $R_{rs}$  signal. To classify the images, we compared the date and time of each SPOT image, with the information contained in historical records of three tide stations of the

**Table 1.** Spectral characteristics of the SPOT sensor bands used in this work. The table shows the spatial resolution in meters of each sensor, the wavelength range of each band and its identifier.

SPOT Sensor	S0 (Blue, 450-520 nm)	S1 (Green, 500-590 nm)	S2 (Red, 610-680 nm)	S3 (Near Infrared (NIR) 780-890 nm)	S4 (Short-Wave Infrared (SWIR) 1580-1750nm)
2 (20 m)		√	√	√	
4 (10 m)		√	√	√	√
5 (10 m)		√	√	√	√
6 (2.5 m)	√	√	√	√	

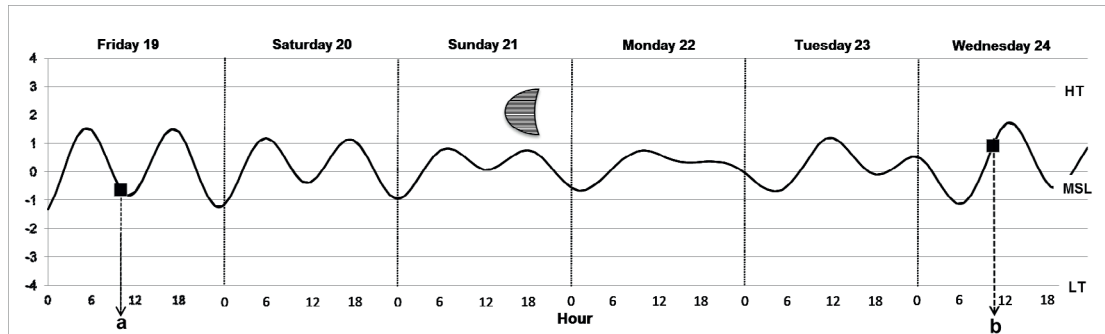


**Figure 2.** Tide behaviour between August 19 and 24, 2011 in Puerto Peñasco. a) SPOT image of August 19, 2011, 9:58 am local time, b) SPOT on August 24, 2011, 10:00 a.m. local time. (HT=High Tides; MSL= Mean Sea Level; LT=Low Tides).

UGC (Golfo de Santa Clara, Puerto Peñasco and San Felipe). The images were grouped in the following way to form mosaics of scenarios:

1) Neap tide (during the first and third quarter moon, when the moon appears “half full”, the sun and moon are at right angles to each other, bulge of the ocean caused by the sun partially cancels out the bulge of the ocean caused by the moon) (e.g. Figure 2) in flux (slow and continuous rise of the waters) or reflux (slow and continuous descent of the waters) (e.g. Figure 3).

2) Spring tide (new and full moon, moon and sun are aligned and their effects are added) in flux or reflux

3) Season, warm or cold season.

The selection of these conditions is justified by the studies of Álvarez-Borrego (1975), Carriquiry *et al.* (1992) and Zamora (1993), that describe the variability of the turbidity patterns in the AGC according to a periodic pattern of semidiurnal character (ups and downs of tides) and a pattern of behaviour that responds to the variation of the tide cycle (neap tide - spring tide - neap tide). The sediment resuspension, caused by the action

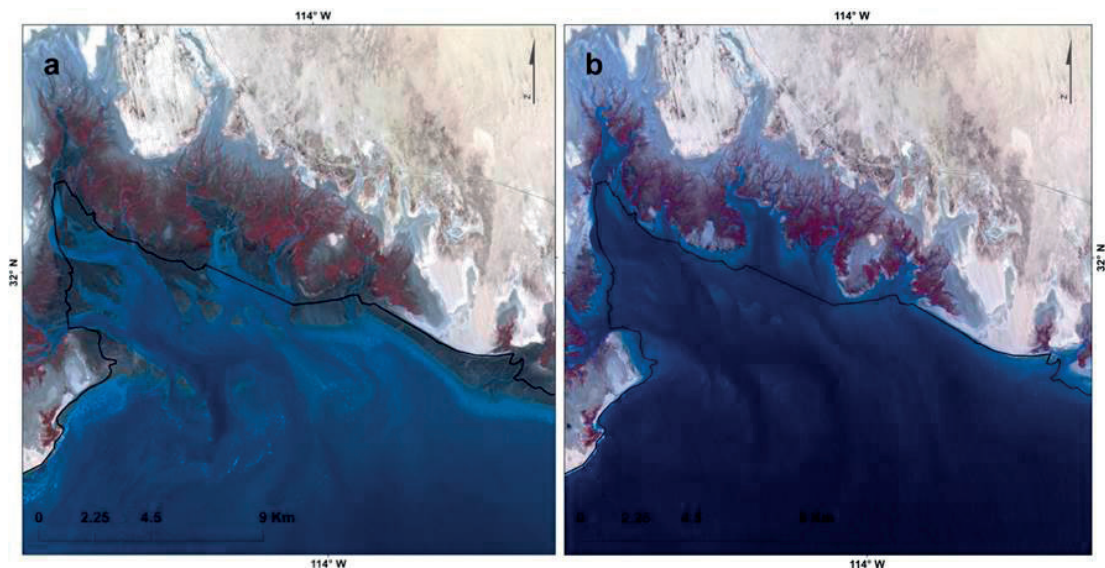


**Figure 3.** SPOT 4 images from Bahía de Adair, Sonora, near to Puerto Peñasco tide station: a) Image of August 19, 2011, 9:58 a.m. local time, at neap tide at reflux, b) Image of August 24, 2011, 10:00 a.m. local time, at neap tide in flux.

of tidal currents, is considered as the governing mechanism of the variability of suspended particulate matter in estuaries (Carriquiry and Sánchez, 1999).

Due to the time when the SPOT scenes were taken, some scenarios were better represented. It was not possible to obtain images of spring tides at reflux, so this condition could not be analysed in this work.

## 2.6. SPOT Association with MODIS

The MODIS band  $M1_{620-670}$  was chosen as the best one to determine areas and levels of turbidity (see results section) (Chen *et al.*, 2007; Chust *et al.*, 2006; Dogliotti *et al.*, 2011; Miller and McKee, 2004). A Match-up analysis was performed to associate SPOT  $R_{rs}(S2_{610-680})$  and MODIS  $R_{rs}(M1_{620-670})$  according to Santamaría-del-Ángel *et al.*, (2011a) methodology. In this analysis, the standardized values were compared in order to deduce the degree of relationship existing between the two types of images and the behaviour of the different levels of  $R_{rs}$ .

The values of the standardized spatial anomalies were classified according to a normal distribution with a known mean and standard deviation (Santamaría-del-Ángel *et al.*, 2015), and according to the methodology Six Sigma, where the upper and lower limits are six standard deviation (SD) (from -3 to +3 SD) (Pyzdek, 2003). In this study, the lower and upper limits were fixed in 2 SD, in order to be able to highlight the in a more visible way, so that values below or above this limit will be highly anomalous values. Values were classified as: “Very Low” less than -2 SD; “Low” between 2 SD to 1 SD; “Medium Low” from -1 SD to 0; “High Medium” ranges from 0 to 1 SD; “High” ranges from 1 SD to 2 SD and “Very High” values greater than 2 SD.

## 2.7. SPOT Association with Secchi Disk Depth

The second step to validate the suitability of SPOT for the detection of turbidity areas was its comparison with *in situ* measurements of Secchi disc depth in the UGC. Measurements were made during boat cruises, in a program called PANGAS conducted by the Phytoplankton Ecology group

of the Autonomous University of Baja California, who attempt to have continuous monitoring at the UGC. These cruises were carried out in the years 2008 (June 3 to 16), 2010 (June 1 to 8), 2011 (March 25 to April 1), 2012 (September 4 to 9) and 2013 (June 11 to 17); in addition to a cruise of the Mexican Navy of 2012 (August 3 to 7) (Figure 4). The values of Secchi disk depth were classified according to the conditions that prevailed at the time of sampling (neap tide or spring tide, warm or cold condition), to be compared with SPOT images at the same conditions.

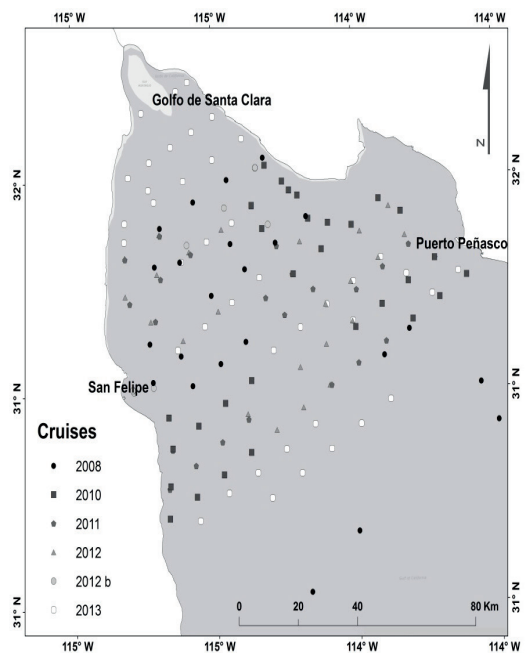


**Figure 4.** Distribution of sampling points during the cruises of 2008, 2010, 2011, 2012 and 2013, where measurements were taken from Zsecchi (2012 b refers to the cruise of the Mexican Navy).

## 3. Results and Discussion

The best association between the SPOT bands was derived from the PC and the correlation matrix, which were calculated as SFEO (Equation 1), where according to the methodology proposed by Santamaría-del-Ángel *et al.* (2011b) the statistically significant SFEO are those with eigenvalues greater than 1.0. Eigenvalues smaller than 1.0 are not significant, and therefore the SFEOs associated with them are not valid because the percentage

of variability explained is infinitesimal. Thus, the first PC in each association was chosen as the component that explains the greatest amount of information.

$$SFEO_i = ((b_{1A} \times S1) + (b_{1B} \times S2) + (b_{1C} \times S3) + (b_{1D} \times S4)) \quad (1)$$

Where  $b_{1A,B,C,D}$  are the eigenvalue of the first PC and  $S1, S2, S3, S4$  are the values of each band that makes up an SPOT image.

Of the 73 SPOT images evaluated according to the described methodology, 69 images had a single significant eigenvalue ( $> 1.0$ ), that is, a single main component explained most of its variability. While, only in 4 of the images evaluated, two significant eigenvalues detected. Of the 69 images in which only one PC was significant, in 68 the sign of the values was the same for the four bands, which corroborates that the bands of the SPOT images are highly associated with each other. In 65 images of the 73 processed (89% of cases analysed), the  $R_{rs}(S2_{610-680})$  was the band with the largest association. Thus, this SPOT band is considered as the best one to represent the reflectance associated to turbidity.

This result is in concordance with previous research done with SPOT in other areas. Doxaran *et al.* (2002), observed that the reflectance increases with the concentration of turbidity, and that the SPOT bands are saturated to higher levels of suspended particles, in the Giron estuary (France). They used  $S1_{550-590}$  y  $S2_{610-680}$  visible bands, to determine turbidity concentrations, this choice of bands is corroborated in the results our PCA analysis. Also, Froidefond *et al.* (1991) used these bands to determine the structure of the turbid plume in this estuary. In particular, they compared the  $S2_{610-680}$  with the turbidity measurements, giving positive results on the variations of thickness of the turbid plume. Finally, in this estuary also Gernez *et al.* (2015), performed a multi-sensor comparison with *in situ* data to observe turbidity variations, and concluded that SPOT data are adequate to detect and quantify turbidity. In contrast, Sánchez-Carnero *et al.*, 2014, used the band  $S1_{550-590}$  in the estuary of the Guadiana (Spain), but mainly in waters slightly turbid.

Thus, in this study, it was possible to corroborate the high redundancy of the different bands in a SPOT scene by other authors, allowing to conclude that all behave in a similar way. However, the  $S2_{610-680}$  was selected because it showed the greatest association in most cases, and also we sought to simplify data processing.

The state of the art of MODIS was revised to define the best band to study turbidity. Dogliotti *et al.*, (2011), used three bands, two in the visible spectrum ( $M1_{620-670}$  and  $M15_{743-753}$ ), and the infrared band  $M16_{862-877}$ . They observed that the reflectance saturation grows at a longer wavelength. In their research, Chust *et al.* (2006) significantly correlated the  $M1_{620-670}$  band reflectivity with the three optical properties (transmittance, Secchi disk transparency and nephelometric turbidity). Miller and McKee (2004) positively related the  $M1_{620-670}$  band with total suspended material concentration, and Chen *et al.* (2007) also showed a close correlation between  $M1_{620-670}$  band and *in situ* turbidity. Thus, the MODIS  $M1_{620-670}$  band was selected as the suitable one to detect turbidity in the water, and therefore the one to be compared with SPOT.

In order to compare SPOT  $R_{rs}(S2_{610-680})$  and MODIS  $R_{rs}(M1_{620-670})$ , was key that both images had the same coverage and pixel number, to create a Pearson correlation matrix. In this step, the zero values associated with the image background were removed. According to the Match-up approach analysis (Santamaría-del-Ángel *et al.*, 2011a), standardized SPOT  $R_{rs}(S2_{610-680})$  values were compared with MODIS  $R_{rs}(M1_{620-670})$ .

Figure 5 shows the distribution of the relationship between these two bands. Two areas are appreciated, one that groups values below 3 Standard Deviations (SD), where the relationship tends towards the linearity, and an area where the anomalies are greater than 3 SD, where the behaviour ceases to be linear and shows a greater accumulation of data towards SPOT  $R_{rs}(S2_{610-680})$ .

The two sets of data were separated to better analyse the relationship between  $R_{rs}(S2_{610-680})$  and  $R_{rs}(M1_{620-670})$ . Data below 3 SD had a Pearson correlation of 0.98 (Figure 6a). A slope analysis was performed based on a linear model, where the rate of change was 1 unit of SPOT  $R_{rs}(S2_{610-680})$  by 0.99 of MODIS  $R_{rs}(M1_{620-670})$ . The significance of the slope was high, it can be observed that there is

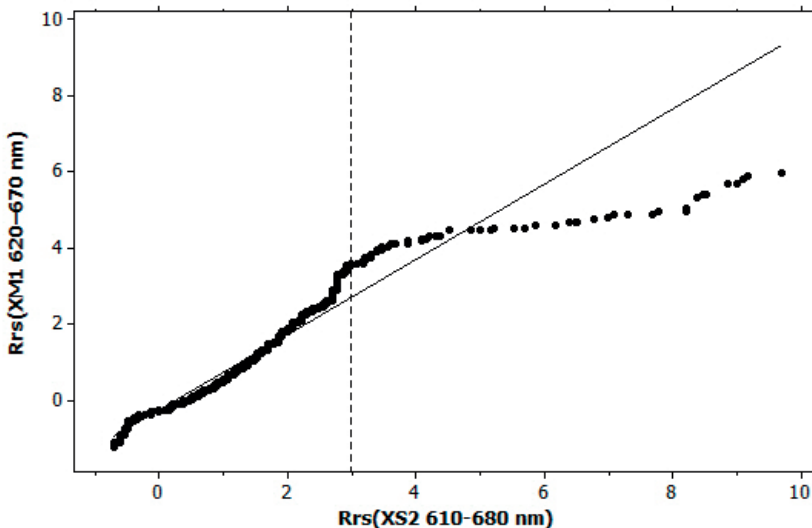


**Figure 5.** Relationship between de MODIS  $R_{rs}(M1_{620-670})$  and SPOT  $R_{rs}(S2_{610-680})$  for the images of February 22, 2012. The data are divided into two groups, values below the 3 SD and values above the 3 SD.

a close relationship between the data of MODIS  $R_{rs}(M1_{620-670})$  and SPOT  $R_{rs}(S2_{610-680})$ . However, data greater than 3 SD had a Pearson correlation of 0.94 (Figure 6b). The rate of change in the slope analysis was 1 unit of SPOT  $R_{rs}(S2_{610-680})$  by 0.38 of MODIS  $R_{rs}(M1_{620-670})$ . The data were indexed to SPOT, which means that in high SPOT reflectances it had lower saturation and responded better.

SPOT  $R_{rs}(S2_{610-680})$  and MODIS  $R_{rs}(M1_{620-670})$  data were classified into  $< 3$  SD and  $> 3$  SD (Figure 5) to better observe the anomalous values distribution. The highly anomalous data corresponded to the intertidal zones for both sensors. However, it is

in MODIS  $R_{rs}(M1_{620-670})$  where there was a greater number of pixels above the 3 SD. This indicates that it is this sensor band the one which has a higher saturation towards the very high  $R_{rs}$ . This anomalously high signal was interpreted as high abundance of particulate material and detritus.

Suspended material predominates in the Colorado River Delta area (CDR) and intertidal zones of the UGC. According to Carriquiry *et al.* (2011), the suspended material is controlled by the hydrodynamic processes that favour a net transport during the flow and the reflux. In addition, fine-grained material is further transported mainly along the

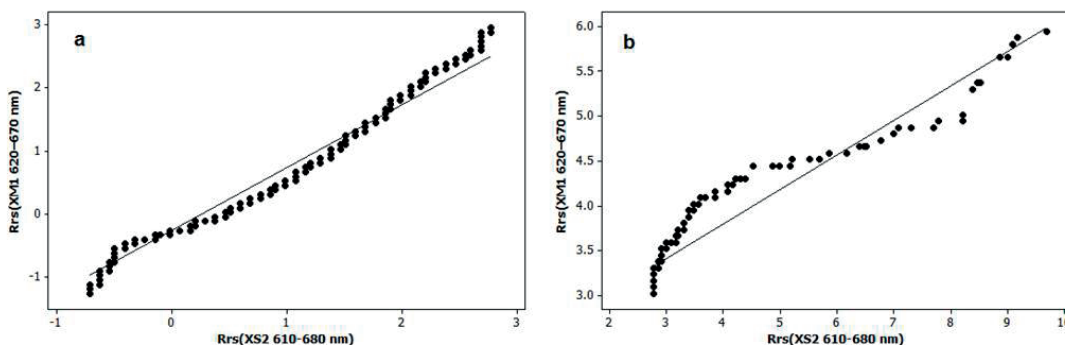


**Figure 6.** Relationship between  $R_{rs}(M1_{620-670})$  and SPOT  $R_{rs}(S2_{610-680})$  for the images of February 22, 2012. Detail of the two data groups, a) values below the 3 SD and b) values above the 3 SD.

coast of Baja California by tidal currents, baroclinic circulation and gravity currents (Carriquiry *et al.*, 1999). Alvarez and Jones (2004), attribute the high concentration of material in suspension to the erosion of bed sediments, since at present the discharge of the Colorado River is insignificant. The amount of particulate material suspended in the water column is controlled by tidal resuspension. The turbidity patterns obtained from the Secchi disk readings indicated that the concentration of suspended material particles shows a persistent southward gradient with the highest values for CDR area and intertidal zone. The research of Aguilar-Maldonado *et al.* (2017), showed the predominance of detritus against coloured dissolved organic matter and phytoplankton in the CDR area. Thus, the observed high reflectances are associated with suspended particulate matter, and higher turbidity.

The relationship between the standardized anomalies of  $R_{rs}(M1_{620-670})$  and  $R_{rs}(S2_{610-680})$ , provided the basis for stating that SPOT had the functionality to observe and discern values of turbidity, since their

relation was always significant. Being significant those results in which the calculated value is greater than or equal to the critical value;  $r \geq r_{critical}$ . The associations based on the Pearson correlation by year and by season (cold or warm) between these two bands, for (n=1000), with different confidence levels (CL), the critical value was: CL 90%=0.052, CL 95%=0.062, CL 99%=0.081, they were in all cases positive relationships.

Secchi's disk depths were interpolated to create a continuous surface from the sampling points values, the method used was nearest neighbour analysis (Sibson, 1981) (e.g. Figure 7). The result were 250 m resolution images of each sampling campaign, which were cut to the area and associated with the scenarios generated with SPOT. The images were classified from "Very Low" (lower depth of disk of Secchi) to "Very High" (greater depth of Secchi in meters). That is in inverse association with turbidity.

SPOT  $R_{rs}(S2_{610-680})$  and Secchi disk depth standardized spatial anomalies were associated using Pearson's correlation coefficient (Santamaría-del-Ángel *et al.*, 2011b). From the standardized values the correlation matrix was obtained, where each cruise was associated to its temporal scenarios (warm or cold season). The critical value that defines the association as significant, according to the Pearson correlation table for a *n* of 1000 and a 95% confidence level, is 0.062 (Table 2). All values of the correlation were above the critical value, which indicates the significant association between the two variables. *In situ* measurements of Secchi disk, during warm conditions, were always performed during neap tides, to prevent the boat to be stranded. Thus in warm conditions the highest correlation occurs in the neap tides. The value of the transparency measured by Secchi disk was used as an estimate of the extinction of light in water (French *et al.*, 1982). The extinction of light in aquatic environments comes from the amount of suspended particles, dissolved pigments and the water's own characteristics (Verduin *et al.*, 1976). Disk Secchi measurements have been related to the concentration of suspended particles and have been used as an indicator of water quality (Santamaría-del-Ángel *et al.*, 2015).

The built scenarios, with mosaics starting from the prompting of the overlapping pixels, from the  $R_{rs}(S2_{610-680})$  allowed to observe the distribution

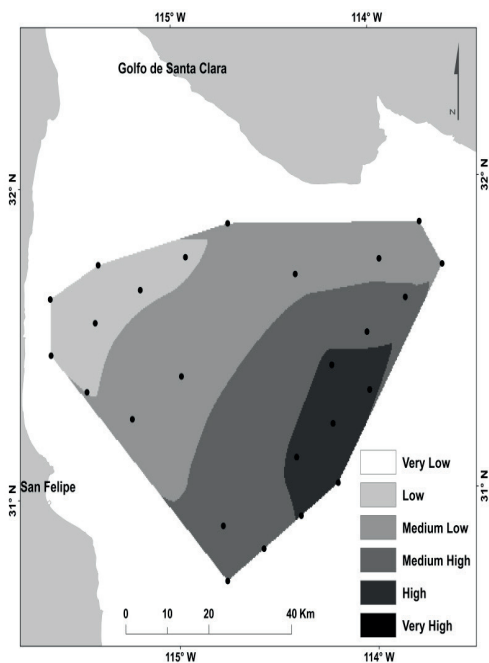


**Figure 7.** Interpolation of Secchi disk data from the 2012 monitoring cruise. The points indicate the location of the sampling stations

**Table 2.** Scenarios built with the depths of Secchi disk, which was associated with the same scenarios built with SPOT. The biggest association by scenario is shaded.

Cruises	Conditions (Scenarios)	Related Pixels ( <i>n</i> )	Correlation	Confidence interval 95%
June 2008	Warm spring tide in flux	63905	0.821	√
	Warm neap tide in flux	65299	0.908	√
	Warm neap tide in reflux	42957	0.813	√
June 2010	Warm spring tide in flux	44722	0.854	√
	Warm neap tide in flux	53145	0.872	√
	Warm neap tide in reflux	29788	0.713	√
March 2011	Cold en spring tide in flux	46588	0.933	√
	Cold neap tide in flux	43192	0.894	√
	Cold neap tide in reflux	39578	0.806	√
September 2012	Warm spring tide in flux	41310	0.840	√
	Warm neap tide in flux	47827	0.917	√
	Warm neap tide in reflux	31547	0.916	√
June 2013	Warm spring tide in flux	89439	0.886	√
	Warm neap tide in flux	97973	0.956	√
	Warm neap tide in reflux	57755	0.940	√

and concentration of the turbidity, in cold conditions (Figure 8) and in warm conditions (Figure 9).

For the cold season the following spatial coverage and turbidity intervals were observed (Figure 8): a) spring tide in flux, spatial coverage was 7275 km<sup>2</sup>, of which 30% had low turbidity; b) neap tide in flux, spatial coverage was 7440 km<sup>2</sup> of which 30% had very low turbidity; and c) neap tide in reflux, spatial coverage was 7027 km<sup>2</sup> of which 38% had medium low turbidity. Thus, during the cold season, the range of turbidity from very low to medium low prevailed in all cases.

For the warm season the following spatial coverage and turbidity intervals were observed (Figure 9): a) spring tide in flux, spatial coverage was 8011 km<sup>2</sup>, of which 24% had low turbidity; b) neap tide in flux, spatial coverage was 5767 km<sup>2</sup> of which 30% had low turbidity; and c) neap tide in reflux, spatial coverage was 5972 km<sup>2</sup> of which 31% had medium low turbidity. Thus, during the warm season, the low range of turbidity prevailed in all cases.

Low turbidity values predominated in all scenarios. However, it is evident from the coverage that the intertidal zone, both in the Adair Bay (Sonora)

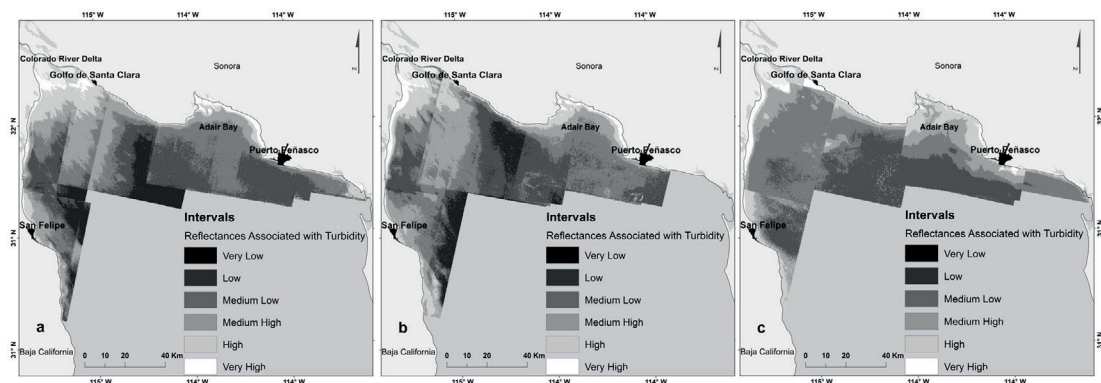


**Figure 8.** Scenarios of turbidity concentration in cold conditions estimated with SPOT  $R_{rs}(S2_{610-680})$ , tide conditions were: a) spring tide in flux, b) neap tide in flux, and c) neap tide in reflux.

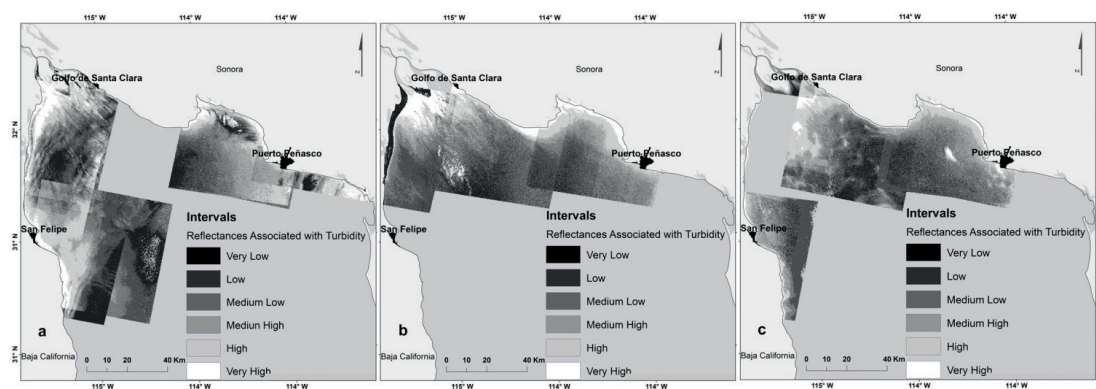


**Figure 9.** Scenarios of turbidity concentration in warm conditions estimated with SPOT  $R_{rs}(S2_{610-680})$ , tide conditions were: a) spring tide in flux, b) neap tide in flux, and c) neap tide in reflux.

and the CRD areas, very high values of turbidity were observed in almost all scenarios (Figure 8 and 9). As the distance from the coast increases the turbidity values decrease, but without reaching the very low values. This high observed turbidity coincides with studies carried out in the area (Carrquirry *et al.*, 1992; Zamora, 1993; Cupul, 1994; Carrquirry and Sánchez, 1999). The high and very high turbidity values are due to two opposite coastal transport components along the Sonora and Baja California coasts. With some local exceptions, sediment transport along the Sonora coast is from SE to NW, and along the coast of Baja California from N to S. This dynamic seems to indicate the existence of a large counter clockwise circulation cell in which sediments transported north along the coast of Sonora drift westward into the delta region and then toward the south along the coast of Baja California.

The AGC and the CRD are considered an extremely turbid place due to sediments resuspension, with Zsecchi values between 0.15 and 1.5 m (Santamaría-del-Ángel *et al.*, 1996), light extinction coefficient as low as  $-0.05 \text{ m}^{-1}$  and a maximum sedimentary load of 8 g/L (Carrquirry and Sánchez, 1999). According to, Carrquirry *et al.* (1992), in general, the concentration of turbidity tends to increase as the tide decreases, because the reduction of the depth in the channel is combined with the intensification of the reflux current, increasing the concentration of sediment in suspension.

In this work, the use of several sensors of the SPOT constellation allowed to raise the temporal resolution, being able to have a greater number of images of smaller time intervals, increasing the coverage and allowing to observe the dynamics of the turbidity in a coastal area with optically complex waters. The time series used in various works related to turbidity and particulate material using low spatial resolution images of ocean colour had, in general, a lower temporal resolution: one or two very specific dates (Shi and Wang, 2007), a pair of images of the same year (Simon and Shanmugam, 2012), two-year series of images with different sensors (Doxaran *et al.*, 2014), monthly images of only one year (Huot and Antoine, 2016); and at the best, time series of two or three years (Chen *et al.*, 2007). With high spatial resolution sensors, the time series observed in other works have also been shorter or sensors have been combined in order to complete larger series (Ruddick *et al.*, 2008; Sánchez-Carnero *et al.*, 2013; Lafon *et al.*, 2014), or even used a single image during their research (Doxaran *et al.*, 2002; Mohd-Hasnadi and Norsaliza, 2010). Our research analysed a 6-year time series with a number of images greater than all the works reviewed. Specifically, the diversity of dates allowed us to observe the turbidity behaviour under a wide variety of scenarios in cold and warm conditions. Even so, some scenarios were incomplete, due to the time of the satellite pass, which is usually at the times when the sun is closer to the zenith, which caused areas to exist uncovered in scenarios that did not match the satellite pass.

The positive association of SPOT  $R_{rs}(S2_{610-680})$  with MODIS and Zsecchi, shows that this SPOT band is suitable for defining patterns and areas of turbidity. The use of satellite imagery does not exclude *in situ* data collection, combining satellite data with field observations improves understanding of turbidity dynamics (Doxaran *et al.*, 2014). Secchi disk data is simple to acquire and the information it provides enables complex analyses of the optical properties of the ocean, such as water turbidity, directly associated with transparency (Santamaría-del-Ángel *et al.*, 2015).

Time series information is basic for taking sound management decisions. Unfortunately, these series are not always available for many parameters, and in the marine environment less than in terrestrial environments due to high costs mainly. This is the case of turbidity. In spite of remote sensing technology advances, we only have short records and more accurate data for oceanic waters than for coastal ones. Cozzoli *et al.* (2017) observed that extensive data series of field collected observations, including both hydromorphological and biological measurements, are virtually never available with an extent that is relevant compared to the morphodynamic scales, which reduces the possibility to fit and field-validate predictive models.

As observed by other researchers, turbidity levels are increasing in many coastal regions due, not only to marine activities, but to terrestrial activities such as large scale land clearance (Gibbs, 2013). However, there is no information, or not enough, about turbidity background levels to be able to discriminate the effects of coastal infrastructures from natural variability or terrestrial origin effects. Environmental monitoring programs of these infrastructures, i.e. ports, prescribe turbidity measures usually during the dredging operations, which is very time limited information (Gibbs, 2013). Coastal environments are characterized by large internal heterogeneity which should be known to reduce the uncertainty in predicting the environmental consequences of new coastal infrastructures. As Cozzoli *et al.* (2017) said: “*the realization of new coastal infrastructure is an unrestrainable need of human society*” and as an example of this, over the past decade, the global dredging market increased by nearly three-fold. This same trend has been observed by other

authors such as Dafforn *et al.* (2015) who highlighted: “*the need for improved defences around ports, harbours, and coastal cities as protection from both rising sea levels and increasingly severe coastal storms and flooding*” or Hill (2015) who added other factors that are likely to increase investments in coastal infrastructure such as higher rates of salinization of water supplies. The effects on the geomorphology and ecology of coastal systems of both the construction and operation phases of these artificial coastal structures is undeniable. The alteration of sediment transport dynamics and turbidity levels can severely affect biotic communities. Thus, is key the development of capacities for acquiring a better knowledge of temporal and spatial patterns. This is what has been tested in this research that the high spatial resolution SPOT sensor offers.

#### 4. Conclusions

The highly turbid waters of the UGC allowed to have a series of contrasting characteristics to test the spectral capacity of the sensors SPOT. The analysis of a six-year series of images allowed to define SPOT  $R_{rs}(S2_{610-680})$  as the optimal band to detect and quantify turbidity in optically complex waters. The Principal Component Analysis proved to be a useful tool to discriminate the most adequate band. The statistically significant relationship of SPOT  $R_{rs}(S2_{610-680})$ , with MODIS  $R_{rs}(M1_{620-670})$  and *in situ* Disk Depth of Secchi validated the suitability of SPOT for turbidity analysis in this type of water. The high spatial resolution of the SPOT sensor allows locating the sediment transport gradients and the accumulation zones, represented by the areas with the highest reflectances. In addition, the high temporal resolution allowed to observe the different conditions of tide and flow, factors with greater influence on turbidity in this type of ecosystems. To evaluate the performance of a specific sensor, the previous classification of images according to oceanographic conditions is a key factor. A good sensor should provide accurate results under all the variability conditions studied. The analysis of different conditions showed that the response of SPOT  $R_{rs}(S2_{610-680})$  is similar to MODIS  $R_{rs}(M1_{620-670})$  for low and medium turbidity concentrations, but for high concentrations the SPOT response was better. Finally, it should be noted that continuous on-site monitoring allowed

a sufficient number of data to validate the remote sensing analysis methodology. Field data are critical to corroborate remote sensing data. Long time series are essential for the study of oceanographic phenomena, such as turbidity patterns.

## References

- Abreu, L. W., Anderson, G.P. 1996. *The MODTRAN 2/3 Report and LOWTRAN 7 Model*. Technical report, Ontar Corp., North Andover, Mass.
- Ackleson, S., Klemas, V., McKim, H., Merry, C. 1985. A comparison of SPOT simulator data with Landsat MSS imagery for delineating water masses in Delaware Bay, Broadkill River and adjacent wetlands. *Photogramm. Eng. Remote Sensing.*, 51(8), 1123-1129.
- Aguilar-Maldonado, J. A., Santamaría-del-Ángel, E., González-Silvera, A., Cervantes-Rosas, O., López-Acuña, L., Gutiérrez-Magness, A., Sebastián-Frasquet, M. T. 2017. Identification of phytoplankton blooms under the index of Inherent Optical Properties (IOP index). *2nd International Electronic Conference on Water Sciences (ECWS-2)*.
- Álvarez-Borrego, S., Flores-Báez, B. P., Galindo-Bect, L. A. 1975. Hidrología del Alto Golfo de California, II. Condiciones durante invierno, primavera y verano. *Ciencias Marinas*, 2(1), 21-36. <https://doi.org/10.7773/cm.v2i1.275>
- Alvarez, L. G., Jones, S. E. 2004. Short-term observations of suspended particulate matter in a macro-tidal, inverse estuary. The Upper Gulf of California. *J. Coast. Res.*, 20(3), 645-654. [https://doi.org/10.2112/1551-5036\(2004\)20\[645:SOOSPM\]2.0.CO;2](https://doi.org/10.2112/1551-5036(2004)20[645:SOOSPM]2.0.CO;2)
- Anji-Reddy, M. 1993. Remote sensing for mapping of suspended sediments in Krishna Bay Estuary, Andhra Pradesh, India. *Int. J. Remote Sens.* 14(11), 2215-2221. <https://doi.org/10.1080/01431169308954030>
- Bastidas-Salamanca, M., González-Silvera, A., Millán-Núñez, R., Santamaría-del-Ángel, E., Frouin, R. 2014. Bio-Optical Characteristics of the Northern Gulf of California during June 2008. *Int. J. Oceanogr.*, 2014. <https://doi.org/10.1155/2014/384618>
- Baeye, M., Quinn, R., Deleu, S., Fettweis, M. 2016. Detection of shipwrecks in ocean colour satellite imagery. *J. Archaeol. Sci.*, 66, 1-6. <https://doi.org/10.1016/j.jas.2015.11.006>
- Berk, A., Anderson, G., Acharya, P., Chetwynd, J., Bernstein, L., Shettle, E., Matthew, M., Adler-Golden, S. 1999. MODTRAN4 User's Manual, Air Force Res. Lab., Hanscom AFB, Mass.
- Cai, L., Tang, D., Li, X., Zheng, H., Shao, W. 2015. Remote sensing of spatial-temporal distribution of suspended sediment and analysis of related environmental factors in Hangzhou Bay, China. *Remote Sens. Lett.* 6(8), 597-603. <https://doi.org/10.1080/2150704X.2015.1062158>
- Carriquiry, J. D., Cupul, M. A. L., Castro C., P.G. 1992. Anomalía en el balance sedimentario del río Colorado? *Geos, (Unión Geofísica Mexicana)*. Vol.12,15.
- Carriquiry, J., Sánchez, A. 1999. Sedimentation in the Colorado River delta and Upper Gulf of California after nearly a century of discharge loss. *Mar Geol.*, 158(1-4), 125-145. [https://doi.org/10.1016/S0025-3227\(98\)00189-3](https://doi.org/10.1016/S0025-3227(98)00189-3)
- Carriquiry, J., Villaescusa, J., Camacho-Ibar, V., Walter Daessle, L., Castro-Castro, P. 2011. The effects of damming on the materials flux in the Colorado River delta. *Environ. Earth Sci.*, 62, 1407-1418. <https://doi.org/10.1007/s12665-010-0626-z>
- Chen, Z., Hu, C., Muller-Karger, F. 2007. Monitoring turbidity in Tampa Bay using MODIS/Aqua 250-m imagery. *Remote Sens. Environ.*, 109, 207-220. <https://doi.org/10.1016/j.rse.2006.12.019>
- Chust, G., Sagarminaga, Y., Borja, A., Valencia, V. 2006. Extracción de propiedades ópticas en aguas costeras del Golfo de Vizcaya mediante MODIS-250 m. *Revista de Teledetección*, 25 Número Especial, 124-128.
- CONANP. 2007. Programa de Conservación y Manejo Reserva de la Biosfera Alto Golfo de California y delta del Río Colorado. Comisión Nacional de Áreas Naturales Protegidas, Secretaría de Medio Ambiente y Recursos Naturales, México,
- Cozzoli, F., Smolders, S., Eelkema, M., Ysebaert, T., Escaravage, V., Temmerman, S., Meire, P., Herman, P. M. J., Bouma, T. J. 2017. A modeling approach to assess coastal management effects on benthic habitat quality: A case study on coastal defense and navigability. *Estuar. Coast. Shelf Sci.*, 184, 67-82. <https://doi.org/10.1016/j.ecss.2016.10.043>
- Cupul, A. L. 1994. *Flujos de sedimentos en suspensión y nutrientes en la cuenca estuarina del Río Colorado*. M.Sc. Thesis. Facultad de Ciencias Marinas. Universidad Autónoma de Baja California. Ensenada, Baja California.
- Dafforn, K. A. Glasby, T. M., Airoidi, L., Rivero, N., Mayer-Pinto, M. Johnston, E. L. 2015. Marine urbanization: an ecological framework for designing multifunctional artificial structures. *Front. Ecol. Environ.*, 13(2), 82-90, <https://doi.org/10.1890/140050>

- Dogiotti, A., Ruddick, K., Nechad, B., Lasta, C. 2011. Improving water reflectance retrieval from MODIS imagery in the highly turbid waters of La Plata river. *Proceedings of VI International Conference. Current problems in optics of natural waters*. St.Petersburg, Russia, September 6-9.
- Doxaran, D., Froidefond, J., Lavender, S., Castaing, P. 2002. Spectral signature of highly turbid waters. *Remote Sensing of Environment*, 81(1), 149-161. [https://doi.org/10.1016/S0034-4257\(01\)00341-8](https://doi.org/10.1016/S0034-4257(01)00341-8)
- Doxaran, D., Castaing, P., Lavender, S. 2006. Monitoring the maximum turbidity zone and detecting fine-scale turbidity features in the Gironde estuary using high spatial resolution satellite sensor (SPOT HRV, Landsat ETM+) data. *Int. J. Remote Sens.*, 27(11), 2303-2321. <https://doi.org/10.1080/01431160500396865>
- Doxoran, D., Lamquin, N., Park, Y., Mazeran, C., Ryu, J., Wang, M., Poteau, A. 2014. Retrieval of the seawater reflectance for suspended solids monitoring in the East China Sea using MODIS, MERIS and GOCI satellite data. *Remote Sens Environ.*, 146, 36-48. <https://doi.org/10.1016/j.rse.2013.06.020>
- French, R. H., Cooper, J., Vigg, S. 1982. Secchi disc relationships. *Water Res. Bull.*, 18, 121-123. <https://doi.org/10.1111/j.1752-1688.1982.tb04538.x>
- Froidefond, J., Castaing, P., Mirmand, M., Ruch, P. 1991. Analysis of the turbid plume of the Gironde (France) based on SPOT radiometric data. *Remote Sens. Environ.*, 36(3), 149-163. [https://doi.org/10.1016/0034-4257\(91\)90053-9](https://doi.org/10.1016/0034-4257(91)90053-9)
- Forget, P., Ouillon, S., Lahet, F., Broche, P. 1999. Inversion of Reflectance Spectra of Nonchlorophyllous Turbid Coastal Waters. *Remote Sens. Environ.*, 68(3), 264-272. [https://doi.org/10.1016/S0034-4257\(98\)00117-5](https://doi.org/10.1016/S0034-4257(98)00117-5)
- Gernez, P., Lafon, V., Lerouxel, A., Curti, C., Lubac, B., Cerisier, S., Barillé, L. 2015. Toward Sentinel-2 High Resolution Remote Sensing of Suspended Particulate Matter in Very Turbid Waters: SPOT4 (Take5) Experiment in the Loire and Gironde Estuaries. *Remote Sens.*, 7(8), 9507-9528. <https://doi.org/10.3390/rs70809507>
- Gibbs, M.T. 2013. Environmental perverse incentives in coastal monitoring. *Marine Pollution Bulletin*, 73, 7-10. <https://doi.org/10.1016/j.marpolbul.2013.05.019>
- Gippel, C. 1995. Potential of turbidity monitoring for measuring the transport of suspended solids in streams. *Hydrol. Process.*, 9(1), 83-97. <https://doi.org/10.1002/hyp.3360090108>
- Gordon, H., McCluney, W.R. 1975. Estimation of the Depth of Sunlight Penetration in the Sea for Remote Sensing, *Appl. Opt.*, 14, 413-416. <https://doi.org/10.1364/AO.14.000413>
- Hernández-Ayón, J.M., Chapa-Balcorta, C., Delgadillo-Hinojosa, F., Camacho-Ibar, V., Huerta-Díaz, M., Santamaría-del-Angel, E., Galindo-Bect, S., Segovia-Zavala, J. 2013. Dynamics of dissolved inorganic carbon in the Midriff Islands region of the Gulf of California: Influence of water masses. *Cienc. Mar.* 39(2), 183-201. <https://doi.org/10.7773/cm.v39i2.2243>
- Howard, R. G., McCluney, W. R. 1975. Estimation of the Depth of Sunlight Penetration in the Sea for Remote Sensing, *Appl. Opt.*, 14(2), 413-416. <https://doi.org/10.1364/AO.14.000413>
- Griffin, M. K., Burke, H. H. K. 2003. Compensation of hyperspectral data for atmospheric effects. *Linc Lab J.*, 14(1), 29-54.
- Huot, Y., Antoine, D. 2016. Remote sensing reflectance anomalies in the ocean. *Remote Sens. Environ.*, 184, 101-111. <https://doi.org/10.1016/j.rse.2016.06.002>
- IOCCG 2000. Remote Sensing of Ocean Colour in Coastal, and Other Optically-Complex, Waters. Shubha Sathyendranath (ed.), *Reports of the International Ocean-Colour Coordinating Group*, No. 3, IOCCG, Dartmouth, Canada.
- Jalón-Rojas, I., Schmidt, S., Sottolichio, A., Bertier, C. 2016. Tracking the turbidity maximum zone in the Loire Estuary (France) based on a long-term, high-resolution and high-frequency monitoring network. *Cont. Shelf. Res.*, 117, 1-11. <https://doi.org/10.1016/j.csr.2016.01.017>
- Kaufmann, Y. J., Wald, A. E., Remer, L. A., Gao, B.-C., Li, R.-R., Flynn, L. 1997. The MODIS 2.1- $\mu\text{m}$  Channel-Correlation with Visible Reflectance for Use in Remote Sensing of Aerosol. *IEEE Transactions on Geoscience and Remote Sensing*. 35, 1286-1298. <https://doi.org/10.1109/36.628795>
- Le Gall A, Janssen, M.A., Lorenz R.D., Paillou P., Wall, S.D., The Cassini Radar Team 2010. Radarbright channels on Titan. *Icarus*. 207(2), 948-958. <https://doi.org/10.1016/j.icarus.2009.12.027>
- Lee, Z. Shang, S., Qi, L., Yan, J., Lin, G. 2016. A semi-analytical scheme to estimate Secchi-disk depth from Landsat-8 measurements. *Remote Sens. Environ.*, 177: 101-106. <https://doi.org/10.1016/j.rse.2016.02.033>
- Lira-Chávez, J. 2010. *Tratamiento digital de imágenes multiespectrales*. Segunda Edición. México. Instituto de Geofísica, Universidad Nacional Autónoma de México.

- Matthew, M., Adler-Golden, S., Berk, A., Richtsmeier, S., Levine, R., Bernstein, L., Acharya, P., Anderson, G., Felde, G., Hoke, M., Ratkowski, A., Burke, H., Kaiser, R., Miller, D. 2000. Status of atmospheric correction using a MODTRAN4-based algorithm. *Proc. SPIE 4049, Algorithms for Multispectral, Hyperspectral, and Ultraspectral Imagery VI*. <https://doi.org/10.1117/12.410341>
- Mercado-Santana, A., Santamaría-del-Ángel, E., González-Silvera, A., Sánchez-Velasco, L., Gracia-Escobar, M., Millán-Núñez, R., Torres-Navarrete, C. 2017. Productivity in the Gulf of California large marine ecosystem. *Environ. Dev.*, 22, 18-29, <https://doi.org/10.1016/j.envdev.2017.01.003>
- Miller, R., McKee, B. 2004. Using MODIS Terra 250 m imagery to map concentrations of total suspended matter in coastal waters. *Remote Sens Environ.*, 93, 259–266. <https://doi.org/10.1016/j.rse.2004.07.012>
- Millán-Núñez, R., Santamaría-del-Ángel, E., Cajal-Medrano, R., Barocio-León, O. 1999. The Colorado River Delta: A high primary productivity ecosystem. *Cienc Mar.*, 25(4), 509-524. <https://doi.org/10.7773/cm.v25i4.729>
- Mohod-Hasmadi, I., Norsaliza, U. 2010. Analysis of SPOT-5 Data for Mapping Turbidity Level of River Klang Peninsular Malaysia. *Appl. Rem. Sens. J.* 1(2),14-18.
- Moore, G. F., Aiken, J., Lavender, S. J. 2010. The atmospheric correction of water colour and the quantitative retrieval of suspended particulate matter in Case II waters: Application to MERIS. *Int. J. Remote Sens.*, 20(9), 1713-1733. <https://doi.org/10.1080/014311699212434>
- NIMA, Department of Defense World Geodetic System 1984. National Imagery and Mapping Agency Technical (NIMA) Report 8350.2, Third Edition, September 1, 2000.
- Nechad, B., Ruddick, K., Park, Y. 2010. Calibration and validation of a generic multisensor algorithm for mapping of total suspended matter in turbid waters. *Remote Sens Environ.*, 114(4), 854-866. <https://doi.org/10.1016/j.rse.2009.11.022>
- Pyzdek, T. 2003. *The Six Sigma Handbook. Revised and Expanded A Complete Guide for Green Belts, Black Belts, and Managers at all Levels*. The McGraw-Hill Companies
- Sánchez-Carnero, N., Ojeda-Zujar, J., Rodríguez-Pérez, D., Marquez-Perez, J. 2013. Assessment of different models for bathymetry calculation using SPOT multispectral images in a high-turbidity area: the mouth of the Guadiana Estuary. *Int. J. Remote Sens.*, 35(2), 493-514. <https://doi.org/10.1080/01431161.2013.871402>
- Santamaría-del-Ángel, E., Alvarez-Borrego, S., Müller-Karger, F. 1994. Gulf of California biogeographic regions based on coastal zone color scanner imagery. *J. Geophys. Res.*, 99(C4), 7411-7421. <https://doi.org/10.1029/93JC02154>
- Santamaría-del-Ángel, E., Millán-Núñez, R., De la Peña, G. 1996. Efecto de la turbidez en la productividad primaria en dos estaciones en el Área del Delta del Río Colorado. *Cienc Mar.*, 22(4), 483-493.
- Santamaría-del-Ángel E., Millán-Núñez, R., González-Silvera, A.M., Cajal-Medrano, R. 2011a. Comparison of *in situ* and Remotely-Sensed Chl-a Concentrations: A Statistical Examination of the Match-up Approach 241-257. Chapter 17 in *Handbook of Satellite Remote Sensing Image Interpretation: Applications for Marine Living Resources Conservation and Management*. Edited by: Jesus Morales, Venetia Stuart, Trevor Platt and Shubha Sathyendranath J. EU PRESPO and IOCCG.
- Santamaría-del-Ángel E., González-Silvera, A., Millán-Núñez, R., Callejas-Jiménez, M., Cajal-Medrano, R. 2011b. Determining Dynamic Biogeographic Regions using Remote Sensing Data 273-293. Chapter 19 in *Handbook of Satellite Remote Sensing Image Interpretation: Applications for Marine Living Resources Conservation and Management*. Edited by: Jesus Morales, Venetia Stuart, Trevor Platt and Shubha Sathyendranath J. EU PRESPO and IOCCG.
- Santamaría-del-Ángel, E., Soto, I., Millán-Núñez, R., González-Silvera, A., Wolny, J., Cerdeira-Estrada, S., Cajal-Medrano, R., Muller-Karger, F., Cannizzaro, J., Padilla-Rosas, Y., Mercado-Santana, A., Gracia-Escobar, M., Alvarez-Torres, P., Ruiz-de-la Torre, M. 2015. Experiences and Recommendations for Environmental Monitoring Programs. Chapter: 4, in *Environmental Science, Engineering and Technology*. Publisher: Nova Science Publishers, Editors: Maria-Teresa Sebastia-Frasquet, pp.32
- Santamaría-del-Ángel, E., Aguilar-Maldonado, J. A., Galindo-Bect, M.S., Sebastia-Frasquet, M.T. 2017. Marine Spatial Planning: Protected Species and Social Conflict in the Upper Gulf of California. Chapter: 16, in *Marine Spatial Planning: Methodologies, Environmental Issues and Current Trends* Publisher: Nova Science Publishers. Editors: Dimitra Kitsiou and Michael Karydis, pp. 25
- Shi, W., Wang, M. 2007. Detection of turbid waters and absorbing aerosols for the MODIS ocean color data processing. *Remote Sens. Environ.*, 110(2), 149-161. <https://doi.org/10.1016/j.rse.2007.02.013>

- Sibson, R. 1981. A Brief Description of Natural Neighbor Interpolation. Chapter 2 in *Interpolating Multivariate Data*, 21–36. New York: John Wiley & Sons.
- Simon, A., Shanmugam, P. 2012. An Algorithm for Classification of Algal Blooms Using MODIS-Aqua Data in Oceanic Waters around India. *Advance in Remote Sensing*, 1, 35-51. <https://doi.org/10.4236/ars.2012.12004>
- Verduin, J. 1982. Components contributing to light extinction in natural waters: Method of isolation. *Archiv. Hydrobiol.*, 93, 303-312
- Wang, M., Shi, W. 2005. Estimation of ocean contribution at the MODIS near-infrared wavelengths along the east coast of the U.S.: Two case studies. *Geophys. Res. Lett.*, 32(13). <https://doi.org/10.1029/2005GL022917>
- Zamora, C., 1993. *Comportamiento del seston en la desembocadura del Rio Colorado, Sonora-Baja California*. Thesis, Facultad de Ciencias Marinas, Universidad Autónoma de Baja California, Ensenada, Baja California.